Eur. Phys. J. D **31**, 477–485 (2004)
DOI: 10.1140/epjd/e2004-00142-y

THE EUROPEAN PHYSICAL JOURNAL D

Copper clusters: electronic effect dominates over geometric effect

Mukul Kabir[1,a], Abhijit Mookerjee[1,b], and A.K. Bhattacharya[2]

[1] S.N. Bose National Centre for Basic Sciences, JD Block, Sector III, Salt Lake City, Kolkata 700098, India
[2] Department of Engineering, University of Warwick, Coventry CV47AL, UK

Received 3rd May 2004
Published online 26 October 2004 –

Abstract. A minimal parameter tight binding molecular dynamics scheme is used to study Cu_n clusters with $n \leq 24$. We present results for relaxed configurations of different symmetries, binding energies, relative stabilities and HOMO-LUMO gap energies for these clusters. Detailed comparison for small clusters $n = 3-9$ with *ab initio* and available experimental results shows very good agreement. Even-odd alternation due to electron pairing and magic behaviour for Cu_2, Cu_8, Cu_{18} and Cu_{20} due to electronic shell closing are found. We found electronic effects, electronic shell closing and electron pairing in the HOMO dominates over the geometrical effect to determine the relative stability of copper clusters. The present results indicate that tight-binding molecular dynamics scheme can be relied on to provide a useful semiempirical scheme in modeling interactions in metallic systems.

PACS. 36.40.Cg Electronic and magnetic properties of clusters – 36.40.Mr Spectroscopy and geometrical structure of clusters – 36.40.Qv Stability and fragmentation of clusters

1 Introduction

Structural and electronic properties of atomic and molecular clusters are the focus of an ever-increasing number of theoretical and experimental studies [1–3]. The issues include different stable and metastable isomeric geometries, binding energies, relative stabilities, gap energies between highest occupied and lowest unoccupied molecular orbitals (HOMO-LUMO), ionization potentials etc. The electronic configuration of the noble metals Cu, Ag and Au are characterized by a closed d shell and a single s valance electron. Due to the similarity in the electronic configuration, noble metal clusters are expected to exhibit certain similarities to the alkali metal clusters, which are well described by the spherical shell model. Apai et al. conducted EXAFS studies of Cu clusters supported on carbon [4]. Similar studies of Au and Ag clusters were carried out by Balerna et al. [5] and Montano et al. [6] These studies indicate, that the localized d-electrons play an important role in the electronic structure. Hence, the d-electrons and their interactions with the extended s-electrons need to be carefully accounted in a proper theoretical treatment of these noble metal clusters.

Calaminici et al. [7] employed the linear combination of Gaussian-type orbitals density functional (LCGTO-DFT) method to study Cu_n, Cu_n^- and Cu_n^+ clusters with $n \leq 5$. Massobrio et al. [8] studied the structures and energetics of small copper clusters with $n \leq 10$. Copper clusters were also investigated using configuration interaction (CI) method by an effective core potential (ECP) for $n \leq 10$ by Akeby et al. [9]. We have employed full-potential muffin-tin orbital (FP-LMTO) technique to study small copper clusters for $n \leq 9$, in our previous communication [10]. But these kind of first-principles methods are limited to small clusters, which are practically computationally expensive for the clusters larger than $n \sim 10$. Copper clusters have also been studied by using various empirical methods. D'Agostino [11] carried molecular dynamics using a quasi-empirical potential derived from a tight-binding approach for ∼1300 copper atoms. More recently, using Gupta potential [12] with geometry optimization by genetic algorithm, Derby et al. [13] studied global minima for Cu_n, Au_n and their alloy clusters in the size range $n \leq 55$. These kind of empirical methods are found to be good to predict the global minima of the clusters but can not predict electronic properties such as shell closing effect for $n = 2, 8, 18, 20, 40, ...$, HOMO-LUMO gap energies and ionization potentials.

Copper clusters have been also investigated through various kind of experiments. Winter et al. [14] indicated through a series of experiments which include mass spectroscopy, oxygen and water absorption, that there is a competition of jellium-like electronic behaviour and icosahedral geometrical closure effects in small copper clusters. Taylor et al. [15] and Ho et al. [16] carried photoelectron

[a] e-mail: mukul@bose.res.in
[b] e-mail: abhijit@bose.res.in

spectroscopy (PES). Katakuse [17] measured ionization potentials for ionic copper clusters and found evidence of electronic shell structure. More recently, Spasov et al. [18] carried threshold collision-induced dissociation experiment (TCID) for cationic copper clusters to measure binding energies.

In recent years empirical tight-binding molecular dynamics (TBMD) method has been developed as an alternative to the first-principles methods. As compared to those *ab initio* methods, the parametrized tight-binding Hamiltonian reduces the computational cost dramatically. The main problem with the semi-empirical TB methods has always been the lack of transferability of its parameters. Menon et al. proposed a minimal parameter TBMD scheme for semiconductors [19] and extended it for the transition metal clusters [20,21] (Ni_n and Fe_n). We shall describe here a similar technique that allows us to fit the parameters of the model from a fully *ab initio*, self consistent local spin-density approximation (LSDA) based FP-LMTO calculation [10] reported earlier by us for the smaller clusters and then make correction for the environment for the clusters to ensure transferability at least to a degree. Our proposed TBMD scheme will allow us to study both the ground state structures as well as ground state energetics as a function of cluster size. Using this TBMD scheme, we shall investigate the ground structures as well as isomers, binding energies, relative stabilities, HOMO-LUMO gap energies and ionization potentials for copper clusters up to $n = 24$. Results for the larger clusters can be found elsewhere [22]. In this communication, our main aim is to show that this tight-binding method is very efficient to study the larger clusters, by a rigorous comparison with other *ab initio* calculations and available experimental results for $n \leq 9$ and using this method we will show the interplay between the electronic and geometric effect, where electronic effect dominates.

2 Computational method

In this section we shall describe the main ingredients of the present tight-binding scheme, whereas more detailed one can be found elsewhere [19,20]. In this TB scheme, the total energy, E, can be written as a sum of three terms

$$E = E_{el} + E_{rep} + E_{bond}. \tag{1}$$

The electronic part, E_{el}, is given by summing over the eigenvalues ϵ_k of the one electron occupied states of the tight-binding Hamiltonian:

$$E_{el} = \sum_{k}^{occ} \epsilon_k n_k, \tag{2}$$

where n_k is the occupation number of the kth state. Here the energy eigenvalues ϵ_k are obtained by solving the orthogonal $9n \times 9n$ TB Hamiltonian including the outermost $3p$, $3d$ and $4s$ electrons. We have used Slater-Koster (SK) scheme [23] to construct the TB Hamiltonian. In this SK scheme, the diagonal matrix elements are configuration independent and the off-diagonal elements have SK type of angular dependence with respect to the separation vector $\mathbf{r}$. Further, these off-diagonal elements are scaled with respect to the interatomic separation r:

$$V_{\lambda,\lambda',\mu} = V_{\lambda,\lambda',\mu}(d)\ S(l,m,n)\ \exp[-\alpha(r-d)], \tag{3}$$

where d is the equilibrium bond length for the fcc bulk copper, $S(l,m,n)$ is the SK type of functions of the direction cosines l, m, n of of the separation vector $\mathbf{r}$ and α is an adjustable parameter ($=2/d$). The values of the parameters $V_{\lambda,\lambda',\mu}$ can be expressed in terms of the universal constants $\eta_{\lambda,\lambda',\mu}$ [24],

$$V_{\lambda,\lambda',\mu}(d) = \eta_{\lambda,\lambda',\mu}\left(\frac{\hbar^2 r_d^{\tau}}{m d^{\tau+2}}\right), \tag{4}$$

where r_d is characteristic length for copper and the parameter $\tau = 0$ for $s-s$, $s-p$ and $p-p$ interactions, $\tau = 3/2$ for $s-d$ and $p-d$ interactions and $\tau = 3$ for $d-d$ interaction. In Table 1, we present the parameter r_d, the on-site energies E_s, E_p, E_d and the universal constants $\eta_{\lambda,\lambda',\mu}$ for Cu [24]. To prevent the p-orbital mixing, we set $E_s = E_d$ and E_p large enough [20]. This choice of our tight-binding parameters reproduces the band structure of the fcc bulk Cu crystal given by Harrison [24].

Table 1. Parameter r_d, on site energies, E_s, E_p and E_d and the universal constants $\eta_{\lambda,\lambda',\mu}$ for Cu [24].

parameter	value	parameter	value
r_d	0.67 Å	$\eta_{pp\pi}$	−0.81
E_s	−20.14 eV	$\eta_{sd\sigma}$	−3.16
E_p	100.00 eV	$\eta_{pd\sigma}$	−2.95
E_d	−20.14 eV	$\eta_{pd\pi}$	1.36
$\eta_{ss\sigma}$	−0.48	$\eta_{dd\sigma}$	−16.20
$\eta_{sp\sigma}$	1.84	$\eta_{dd\pi}$	8.75
$\eta_{pp\sigma}$	3.24	$\eta_{dd\delta}$	0.00

The second term in equation (1), E_{rep}, is a repulsive term which includes the ion-ion repulsive interaction and a correction term due to the double counting of the electron-electron interaction in the electronic term E_{el}. Here, E_{rep} can be written as a sum of short-ranged repulsive pair potentials, ϕ_{ij}, and scaled exponentially with interatomic distance:

$$\begin{aligned} E_{rep} &= \sum_i \sum_{j,(>i)} \phi_{ij}(r_{ij}) \\ &= \sum_i \sum_{j,(>i)} \phi_0\ \exp[-\beta(r_{ij}-d)], \end{aligned} \tag{5}$$

where r_{ij} is the distance between the atoms i and j and β is a parameter ($= 4\alpha$).

The third term, E_{bond}, in equation (1) is a coordination-dependent correction term introduced by Tomaňek and Schluter [25] for Silicon clusters. It is needed because the first and second terms in equation (1) is not

sufficient to exactly reproduce the cohesive energy of the dimer through the bulk structure. This coordination dependent term is given by,

$$E_{bond} = n\left[a\ \left(\frac{n_b}{n}\right)^2 + b\ \left(\frac{n_b}{n}\right) + c\right], \tag{6}$$

where n is the number of the atoms in the cluster and n_b is the number of bonds in the cluster. As we use a smooth function for the cutoff distance, r_c, for the interactions, n_b can be determined by,

$$n_b = \sum_i \left[\exp\left(\frac{r_{ij} - r_c}{\Delta}\right) + 1\right]^{-1}, \tag{7}$$

where the sum is over all bonds in the cluster. It should be noted that this coordination dependent correction term, E_{bond}, to the total energy does not contribute to the force. It is added to the total energy only after the relaxation has been achieved. However, for metal clusters, this correction term is significant in distinguishing various isomers for a given cluster.

In the present scheme we have four adjustable parameters, ϕ_0 in equation (5) and a, b, c in equation (6). The vale of ϕ_0 is fitted to reproduce the correct experimental bond length for the Cu dimer (2.22 Å [27]). In the present case we found a value 0.34 eV for ϕ_0. We found the vibrational frequency of Cu_2 is to be 226 cm^{-1}, which has reasonable agreement with the experimental value (265 cm^{-1}) [26]. The parameters, a, b and c, are obtained by fitting the coordination dependent term to the *ab initio* results for the three different small clusters according to the equation

$$E_{bond} = E_{ab\ initio}\ - E_{el} - E_{rep}. \tag{8}$$

To determine the parameters a, b and c, we use the experimental binding energy (1.03 eV/atom [27]) of Cu_2 and binding energy of Cu_4 and Cu_6 from our previous *ab initio* FP-LMTO calculation. This gave $a = -0.0671$ eV, $b = 1.2375$ eV and $c = -3.042$ eV. In the present case we took the cutoff distance $r_c = 3.5$ Å and $\Delta = 0.1$ Å. These four parameters, once adjusted for small clusters to reproduce the known experimental or theoretical results, are then kept fixed in the subsequent calculations for clusters of arbitrary size.

The first two terms in equation (1), E_{el} and E_{rep}, contribute to the force only. In particular, the force $\mathbf{F}_i$ acting on the ith atom is

$$\mathbf{F}_i = -\sum_i \langle\psi_i|\nabla_{\mathbf{r}i}H|\psi_i\rangle\ -\ \nabla_{\mathbf{r}i}E_{rep}. \tag{9}$$

In the the above equation, the first term is the Hellmann-Feynman contribution to the total force calculated by spatial derivatives of the TB Hamiltonian H and the second term is the short ranged repulsive force. It should be noted here that Pulay force does not play any role in any semi-empirical TBMD. The reasons are within TBMD scheme, (i) we directly compute the derivative of the TB Hamiltonian matrix element and (ii) the basis wavefunctions never appear explicitly, rather they are implicitly contained in the fitted matrix entries.

Molecular dynamics can be performed by numerically solving the Newton's equation for each component of the force,

$$m\ \frac{d^2x_i}{dt^2} = F_{ix}, \tag{10}$$

where m is the atomic mass of copper.

For numerical simulation of Newtonian dynamics, we use the velocity Verlet molecular dynamics algorithm for updating the atomic coordinates and velocities, which is given by,

$$\mathbf{r}_i(t+\delta t) = \mathbf{r}_i(t) + \mathbf{v}_i(t)\ \delta t + \frac{1}{2m}\mathbf{F}_i(t)\ (\delta t)^2 \tag{11}$$

and

$$\mathbf{v}_i(t+\delta t) = \mathbf{v}_i(t) + \frac{1}{2m}[\mathbf{F}_i(t) + \mathbf{F}_i(t+\delta)]\ \delta t \tag{12}$$

where $\mathbf{v}_i(t)$ and $\mathbf{F}_i(t)$ are the velocity and acceleration of the ith atom at time t.

Here we use dissipative molecular dynamics. For the numerical integration of Newton's equations of motion, we have to choose a finite time-step δt, ideally which should be very small. However, this would require an excessively long time for locating the global minimum and a large choice of δt leads to unphysical heating up of the system, leading to instability. To overcome this difficulty, we add a small extra friction term carefully, $\mathbf{F} \Rightarrow \mathbf{F} - \gamma m\dot{\mathbf{r}}$, which is used by many authors. In the present calculation we took $\gamma m = 0.32$ amu/ps, $\delta t = 1$ fs and the total time for molecular dynamics simulation is ∼100−200 ps, depending upon the cluster size and the initial cluster configuration within the several annealing schedule.

3 Results

By using TBMD method, we studied the lowest energy structures of Cu_n clusters for $n \leq 24$. The minimum energy structures of Cu_n with various isomers for $n = 3-9$ are shown in Figure 1 and the minimum energy structures for $n = 10-24$ are shown in Figure 2. We also studied binding energy, relative stability and highest occupied-lowest unoccupied molecular orbital (HOMO-LUMO) gap of copper clusters. In Table 2, we present binding energy, difference in cohesive energy ΔE and average bond length $\langle r\rangle$ for the ground state structure and the isomers for small clusters with $N \leq 9$. We have compared our results for small Cu_n clusters ($n \leq 9$) with *ab initio* and available experimental results. We found reasonable agreement, which allow us to study the clusters with $n \geq 10$. The details are discussed in this section.

3.1 Most stable structures

3.1.1 The smaller clusters of 3–9 atoms

We carried molecular dynamics starting from various different structures. A straight-forward molecular dynamics

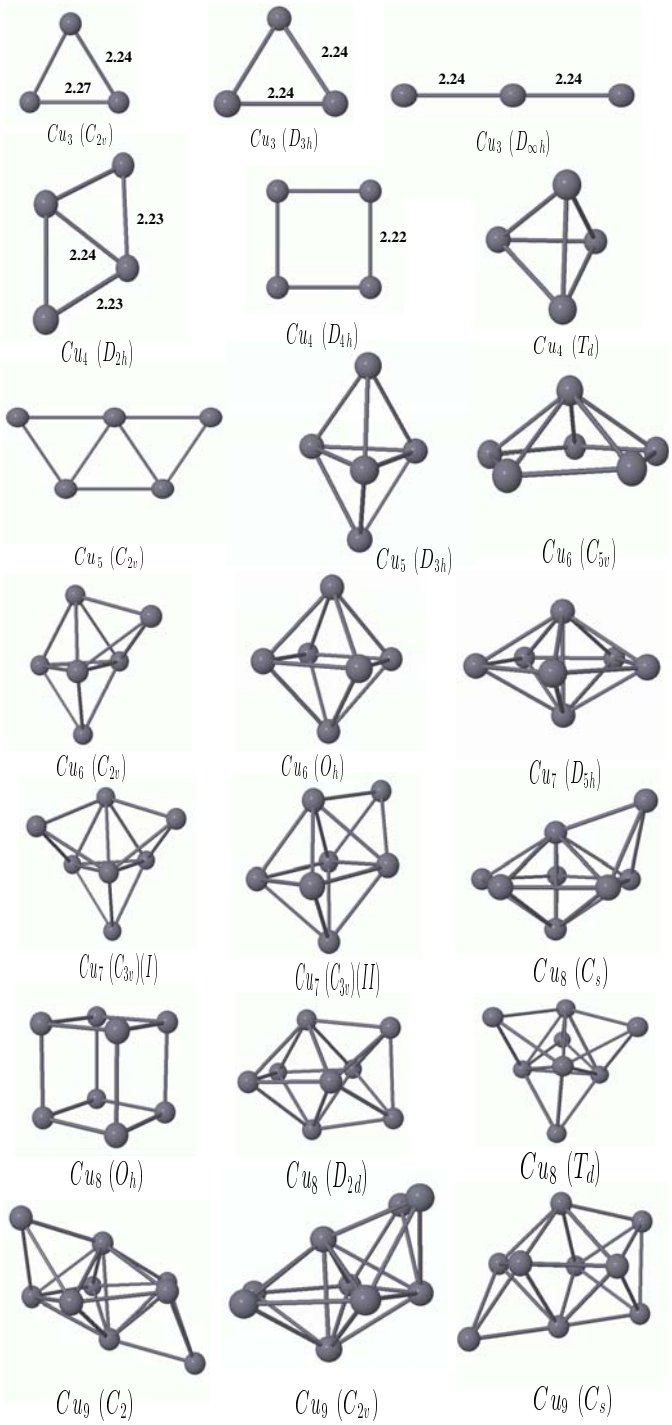

Fig. 1. Ground state structure and isomers of Cu_n clusters for $n = 3-9$. Point group symmetries are given in the parentheses.

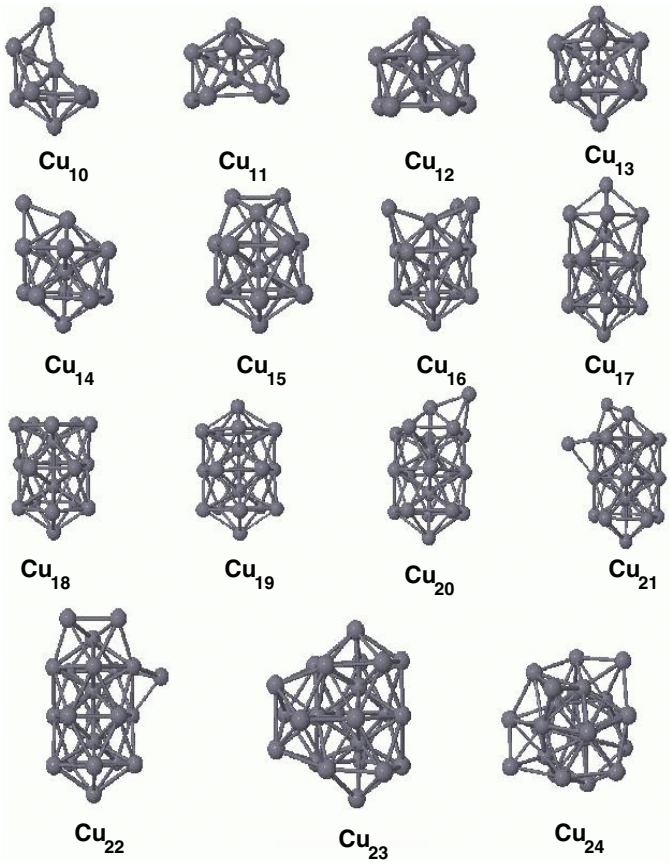

Fig. 2. Ground state structures for the cluster $n = 10-24$. Icosahedral growth is found.

will then lead to possibly a metastable structure. These are the isomers described in the following text. Of these isomers only one has the globally minimum energy. Since the present scheme imposes no a priori symmetry restrictions, we can perform full optimization of cluster geometries.

For the Cu_3 cluster we find the isosceles triangle with C_{2v} symmetry to be the most stable structure. In the present calculation the equilateral triangle (D_{3h} symmetry) and the linear structure ($D_{\infty h}$ symmetry) are the two isomers which are 0.11 eV/atom and 0.30 eV/atom lower in energy. Due to the Jahn-Teller distortion C_{2v} structure is energetically more favourable than the more symmetrical D_{3h} structure. This result is supported by the experimental study of Ho et al. [16], who found the C_{2v} and D_{3h} structures are nearly degenerate. Akeby et al. [9] reported an energy difference of 0.11 eV between the D_{3h} and $D_{\infty h}$ structures, which is 0.23 eV according to *ab initio* calculation [28]. In agreement with the present calculation Lammers et al. [29] also found the isosceles triangle (C_{2v}) to be the the most stable structure, which is 0.16 eV and 0.35 eV higher than the D_{3h} and $D_{\infty h}$ isomers respectively. Calaminici et al. [7] found the vertex angle to be 66.58°, whereas it was 65° in our previous *ab initio* calculation [10]. In the present calculation we find it to be 61.3°.

For the Cu_4 cluster our calculation predict the planer rhombus (D_{2h}) geometry to be the most stable with cohesive energy 2.00 eV/atom. We fond the two isomers, a perfect square (D_{4h} symmetry) and a tetrahedron (T_d symmetry), with cohesive energy 1.73 eV/atom and 1.46 eV/atom respectively. Experimental study [16] also favours the rhombic structure. Hückel calculations [30] suggest the rhombic geometry for the both Cu_4 and Cu_4^-. Our prediction is exactly supported by Akeby

Table 2. Point group (PG) symmetry, cohesive energy per atom, and average bond length $\langle r \rangle$ of the ground state structure and different isomers for Cu_n clusters with $n \leq 9$ obtained from present TB calculation and comparison with *ab initio* calculations, FP-LMTO [10] and DF-LDA [8]. and TCID experimental values [18].

cluster	PG symmetry	binding energy (eV/atom) present	theory FP-LMTO(DF-LDA)	experiment reference [18]	$\langle r \rangle$ (Å)
Cu_3	C_{2v}	1.43	1.60(1.63)	1.07±0.12	2.25
	D_{3h}	1.32			2.24
	$D_{\infty h}$	1.13			2.24
Cu_4	D_{2h}	2.00	2.00(2.09)	1.48±0.14	2.23
	D_{4h}	1.73			2.22
	T_d	1.46			2.24
Cu_5	C_{2v}	2.24	2.19	1.56±0.15	2.23
	D_{3h}	2.03			2.38
Cu_6	C_{5v}	2.54	2.40(2.49)	1.73±0.18	2.40
	C_{2v}	2.40			2.39
	O_h	1.98			2.41
Cu_7	D_{5h}	2.63	2.65	1.86±0.22	2.41
	$C_{3v}(I)$	2.50			2.63
	$C_{3v}(II)$	2.30			2.45
Cu_8	C_s	2.87	2.73(2.84)	2.00±0.23	2.41
	O_h	2.64			2.61
	D_{2d}	2.57			2.59
	T_d	2.51			2.39
Cu_9	C_2	2.87	2.80		2.44
	C_{2v}	2.84			2.59
	C_s	2.60			2.41

et al. [9] and Calaminici et al. [7], who also predicted the sequence D_{2h}–D_{4h}–T_d of decreasing stability. In our previous *ab initio* calculation [10] we found the same sequence, whereas Lammers et al. [29] found a different sequence, T_d–D_{2h}–D_{4h}. The larger angle of the rhombus predicted 123° by Calaminici et al. [7] agrees well with the present calculation 119.8°, which was 120° in our previous *ab initio* calculation [10].

In the case of the pentamer, Cu_5, three different structures were examined, viz., the square pyramid (C_{4v} symmetry), the trigonal bipyramid (D_{3h} symmetry) and the trapezoid (C_{2v} symmetry). Among these three different structures, we found the the planer trapezoidal C_{2v} structure to be the most stable, which is $\Delta E = 0.21$ eV/atom higher than the D_{3h} structure. In our simulation, the square pyramid C_{4v} was found to be unstable, relaxing to a D_{3h} structure. In the photoelectron spectroscopy [16] of Cu_n^-, Ag_n^- and Au_n^-, Ho et al. tentatively assign the trapezoidal planer geometry to the ground state of both the anion and neutral of the coinage metal pentamers. Present result doesn't agree with our previous *ab initio* calculation, where we found the D_{3h} structure to be the most stable but agrees with Calaminici et al. [7] and Akeby et al. [9], both of them found the C_{2v} structure to be most stable structure with the sequence C_{2v}–D_{3h}–C_{4v} of decreasing stability. Lammers et al. found an opposite sequence C_{4v}–D_{3h}–C_{2v}.

For the Cu_6 cluster we investigated three different structures, the octahedron (O_h symmetry), the capped trigonal bipyramid (C_{2v} symmetry) and the flat pentagonal pyramid (C_{5v} symmetry). Among these three structures, we found the flat pentagonal pyramid C_{5v} to be the most stable with cohesive energy 2.54 eV/atom. We found the two isomers, the capped trigonal bipyramid C_{2v} and the octahedron O_h, are $\Delta E = 0.14$ eV/atom and $\Delta E = 0.56$ eV/atom lower respectively. Massobrio et al. [8] and Akeby et al. [9] also found the C_{5v} structure as the ground state. This result does not agree with our previous *ab initio* calculation, where we found the C_{2v} structure as ground state. Lammers et al. [29] predict the O_h structure to be the most stable structure compared to other random structures.

In the case of Cu_7 cluster we considered three different structures, the pentagonal bipyramid (D_{5h} symmetry), the bicapped trigonal bipyramid (C_{3v}(I) symmetry) and the capped octahedron (C_{3v}(II) symmetry), as our initial starting configurations. We found the pentagonal bipyramid with D_{5h} symmetry to be the most stable, which is energetically more favourable than the bicapped trigonal pyramid and capped octahedron isomers by an energy $\Delta E = 0.13$ eV/atom and $\Delta E = 0.33$ eV/atom respectively. This result agrees well with Akeby et al. [9] and with the previous *ab initio* [10] calculation.

For the Cu_8 cluster, we examined four different structures, viz., the capped pentagonal bipyramid (C_s symmetry), the tricapped trigonal bipyramid (T_d symmetry), the bicapped octahedron (D_{2d} symmetry) and the cube (O_h symmetry). In our simulation, we found the capped

pentagonal bipyramid (C_s) to be the most stable with cohesive energy 2.87 eV/atom. We found the three isomers, O_h, D_{2d} and T_d, are lower in energy by $\Delta E = 0.23, 0.30$ and 0.36 eV/atom respectively. This result agrees with our previous *ab initio* calculation [10], where we found the C_s structure to be the most stable but with a different sequence C_s–D_{2d}–O_h with decreasing order of stability. In that study we have not studied the T_d structure. Massobrio et al. [8] found the D_{2d} structure to be the most stable structure followed by T_d and C_s structure.

For the Cu_9 cluster, we examined three different structures, the tricapped octahedron (C_s symmetry), the bicapped pentagonal bipyramid (BPB) with capping atoms on the adjacent faces (C_{2v} symmetry) and the BPB with capping atoms on the non adjacent faces (C_2 symmetry). Among these three structures, the BPB with capping atom on the non adjacent faces was found to be most stable with binding energy 2.87 eV/atom. This C_2 structure is nearly degenerate with the C_{2v} structure by an energy difference $\Delta E = 0.03$ eV/atom, whereas the C_s structure is less stable by an energy difference $\Delta E = 0.27$ eV/atom from the C_2 structure. Zhao et al. [32] found a BPB with C_{2v} symmetry to be the ground state for Ag_9 cluster. In our previous *ab initio* calculation [10], we found the tri-capped octahedron to be the ground state.

3.1.2 Clusters of 10–24 atoms

From the present results and the detail comparisons with various *ab initio* and available experimental results, we find reasonable agreement between the TB model and the *ab initio* calculations for small clusters with $N \leq 9$. This agreement allow us to continue the use of this TB method for larger clusters with $N \geq 10$. For these large clusters, a full configurational space search is not possible within the computational resources. Instead we examined these clusters starting form different initial geometries with different annealing schedule. The most stable structure for Cu_{10} is a tri-capped pentagonal bipyramid which is energetically more favourable than the D_{4d} structure by $\Delta E = 0.08$ eV/atom. The ground state structures start icosahedral packing from Cu_{11}. The ground state structure of Cu_{11} and Cu_{12} are the uncompleted icosahedron with lack of one and two atoms respectively and a Jahn-Teller distorted complete icosahedron (I_h symmetry) is formed at Cu_{13}. For Cu_{13} the fcc like cuboctahedron is less stable than the icosahedron by an energy 0.05 eV per atom. This cuboctahedron consists of a central atom and its 12 first neighbours in a fcc packing structure. Lammers et al. [29] also found the icosahedron to be the most stable for Cu_{13}. The icosahedral growth continues and forms a complete double icosahedron for Cu_{19}, which can be viewed as two interpenetrating 13-atom icosahedron. The ground state structures for Cu_{14}, Cu_{15}, Cu_{16} and Cu_{17} are the single icosahedron capped with 1, 2, 3 and 4 atoms respectively and for Cu_{18} it is a truncated icosahedron. The ground state structures of Cu_{20} and Cu_{21} are the double icosahedron capped with 1 and 2 atoms. A "triple icosahedron" with D_{3h} symmetry is found to be the most stable structure for Cu_{23}. On the each of the three lobes of this cluster four six-coordinate atoms protrude, each having local pentagonal symmetry. Between the lobes are two eight-coordinate atoms and along the central axis of the cluster sit two nine-coordinate atoms. Singly capped triple icosahedron is found to be the ground state for Cu_{24}. So all these clusters in this size range, $10 \leq n \leq 24$, have structures which can be derived from the 13-atom icosahedron, 19-atom double icosahedra or 23-atom triple icosahedra by simply adding or removing atoms from them. This icosahedral growth of copper clusters is supported by the experimental study of Winter et al. [14]. Very recently a study [13] using genetic algorithm with Gupta potential [12], Darby et al. found similar structures for *global minima* of Cu_{10} to Cu_{21} except for Cu_{10}, Cu_{17} and Cu_{18} clusters, which are slightly different from the present calculation. Similar kind of icosahedral growth is found for Ag_n with $n = 11-21$, except at Ag_{14} [32]. In the molecular absorption experiment Parks et al. [33] also found the icosahedral growth for all the clusters ranging from Ni_{16} to Ni_{28}.

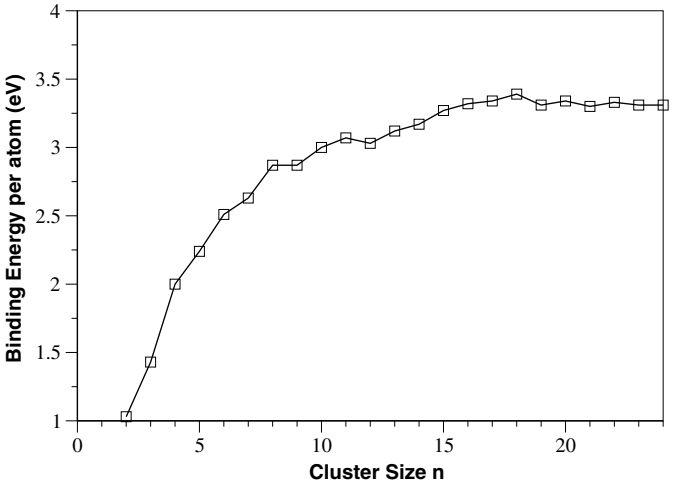

Fig. 3. Binding energy per atom as a function of cluster size n.

3.2 Binding energies

The size dependence of the binding energy per atom for clusters with $n = 2-24$ is depicted in Figure 3. The highest binding energy has been considered for a particular cluster having certain number of atoms for Figures 3 and 4. Binding energy grows monotonically with increasing the cluster size n. For cluster sizes $n = 2-10$, we have compared our binding energies with our previous *ab initio* FPLMTO calculations [10] and also with DF-LDA calculations [8] and TCID experiment [18]. Figure 4 shows that the binding energies match very well with both the *ab initio*, FPLMTO and DF-LDA, calculations but systematically overestimate it form the TCID experiment by an amount 0.53 ± 0.12 to 0.79 ± 0.22 eV. Experimentally the binding energies of neutral copper cluster were

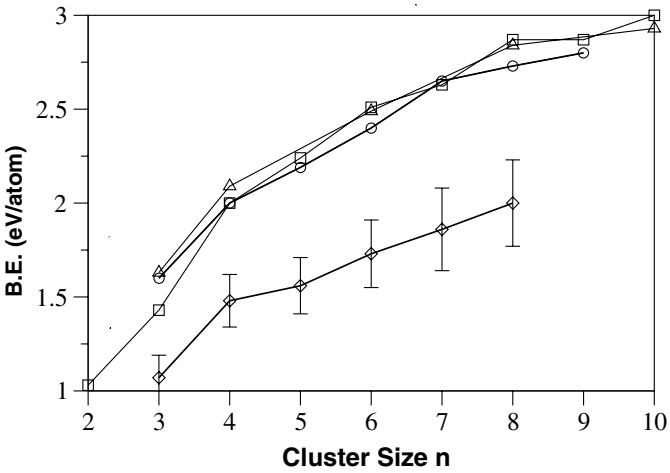

Fig. 4. Comparison of binding energies, calculated from the present TB method (□), with the FP-LMTO (○), DF-LDA (Δ) and TCID experimental (◇) values, for $n = 2-10$ clusters. Calculated binding energies match very well with both the *ab initio*, FP-LMTO and DF-LDA, calculations but systematically overestimate from the TCID experiment. See text for details.

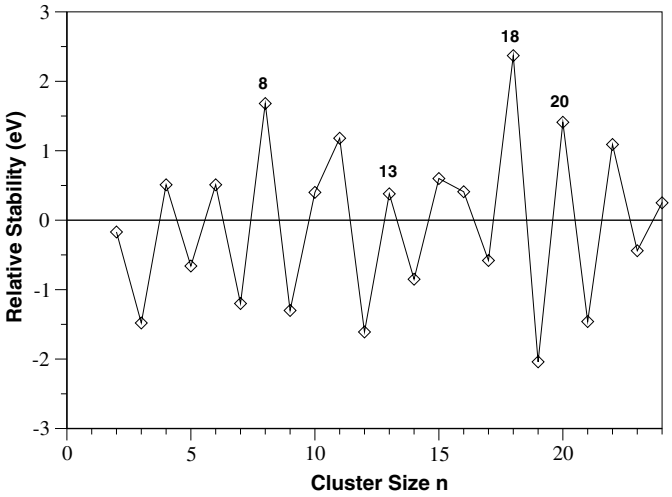

Fig. 5. Relative stability, $\Delta_2 E(n)$ $(= E(n+1) + E(n-1) - 2E(n))$, as a function of cluster size n. Even-odd alternation and pronounced peaks for $n = 8$, 18 and 20 is found. However, due to geometrical effect even-odd alternation is disturbed for $n = 11$, 13 and 15. See text for details.

derived from TCID experiment of anionic clusters and using electron affinities from the PES experiment [16]. As in the present TBMD method, the parameters have been fitted to the Local Density Approximation (LDA) based *ab initio* calculation [10], so this kind of overestimation in the binding energy is not surprising. Rather this is a characteristic of LDA.

3.3 Relative stabilities

The relative stability, which is the second differences of cluster binding energies, is plotted in Figure 5. The relative stability is defined as

$$\Delta_2 E(n) = E(n+1) + E(n-1) - 2E(n). \qquad (13)$$

The relative stability, $\Delta_2 E(n)$, can be directly compared to the experimental relative abundance. Figure 5 shows relative stability as a function of cluster size n, where we found three distinct features. (a) Even-odd alternation (even $>$ odd) for $n = 2-9$, $17-20$, which is due to the electron pairing effect resulting from the fact that each copper atom in the cluster contributes a single valence electron to the bonding orbitals. Even (odd) clusters have an even (odd) number of electrons and the HOMO is doubly (singly) occupied. The electron in a doubly occupied HOMO will feel a stronger effective core potential because the electron screening is weaker for the electrons in the same orbital than for inner shell electrons. Thus the binding energy of the valence electron with an even cluster is larger than of an odd one, which reflects through the even-odd alteration in the relative stability $\Delta_2 E(n)$. (b) We found particular high peak at Cu_8, Cu_{18} and Cu_{20}. This is due to the electronic shell closing at $n = 8$, 18, and 20 which corresponds to the magic number in electronic shell model. Electronic shell structure in coinage metal clusters was first observed by Katakuse et al. [17]. But we have not seen the magic behaviour at Cu_2 in our calculated relative stability. (c) We found even-odd alteration is reversed for $n = 10-16$ with maxima at odd sized clusters, Cu_{11}, Cu_{13} and Cu_{15}, which manifests the geometrical effect through icosahedral growth. Simultaneous appearance of these three features in $\Delta_2 E(n)$ demonstrates that the structure and stability of copper cluster is determined by both electronic structure and atomic configuration. This argument is supported by Winter et al. [14]. In their experiment they found both the jellium-like electronic behaviour and icosahedral geometrical structure of copper cluster.

Using Gupta potential, Darby et al. [13] found significant peaks in the second difference at $n = 7, 13, 19$ and 23, due to icosahedral or poly-icosahedral structure. The Cu_7 has a pentagonal bipyramidal symmetry, which is a building block of icosahedron. In comparison, in the present study we have not found any such peaks due to icosahedral geometrical growth except at $n = 13$. However, we get similar structures predicted by Darby et al. for these clusters. Reason for not getting these peaks due geometrical effect is, the Gupta potential is an empirical potential and can not predict any such electronic effects, whereas the present TBMD can predict both geometrical and as well as electronic effects together. In the present study, we found significant peaks at $n = 8, 18$ and 20 due to electronic shell closing and average (even-odd alternation) peaks at $n = 6, 20$ and 22 for electronic pairing effect. For this reason, peaks due to geometrical (icosahedral or poly-icosahedral growth) structure at $n = 7, 19$ and 23 are suppressed by the peaks at $n = 6, 8, 18, 20, 22$ and 24 due to electronic structure. Therefore in this section, we conclude that electronic effects, electronic shell closing and electron pairing in the HOMO, dominates over

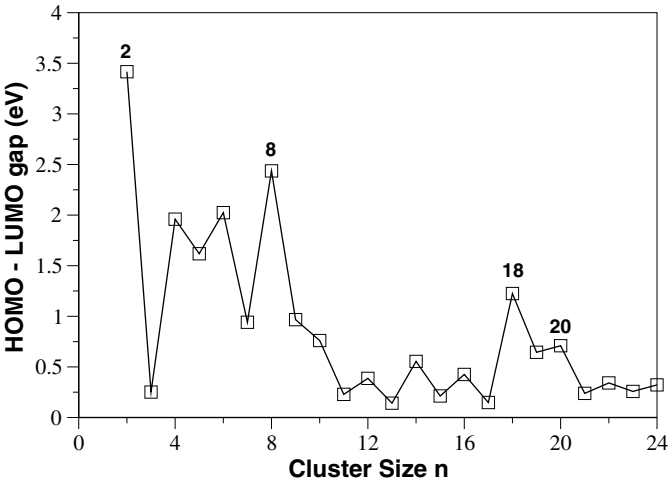

Fig. 6. HOMO-LUMO gap energy as a function of cluster size n.

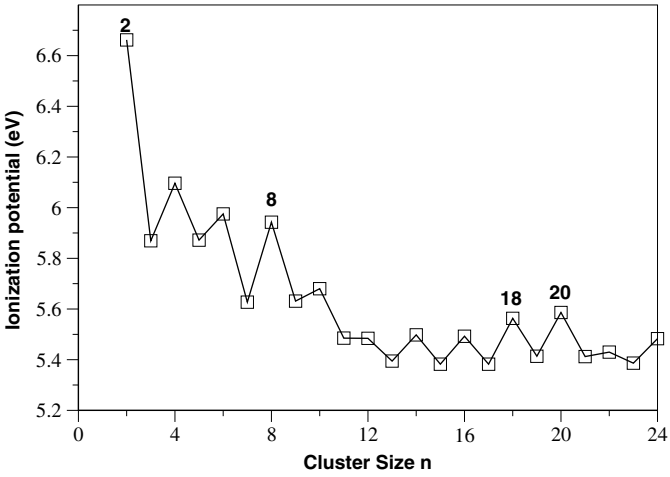

Fig. 7. Ionization potential as a function of cluster size n.

geometrical effect to determine the relative stabilities of the copper clusters.

3.4 HOMO-LUMO gaps

We studied the gap energy between the highest occupied molecular orbital (HOMO) and lowest unoccupied molecular orbital (LUMO), which is a sensitive quantity to probe stability. In Figure 6, we plotted HOMO-LUMO gap energy as a function of cluster size. In the studied region, we found particularly large HOMO-LUMO gap for Cu_2, Cu_8, Cu_{18} and Cu_{20} due to electronic shell closing effect. This was well established by the experiments carried out by Pettiette et al. [34] and Ho et al. [16], where the manifestation of electronic shell closing was found through the particular high peaks in the HOMO-LUMO gap energy. We also found even-odd alternation due to the electron pairing effect. Christensen et al. [35] have studied copper clusters with 3−29 atoms using the effective medium theory and found the clusters with 8, 18 and 20 atoms to be particularly stable. In a previous *ab initio* study of copper clusters [29], the maximum gap at Cu_8 and Cu_{20} is found but even-odd alternation and magic effect for Cu_2 and Cu_{18} have not been obtained. As compared to the experimental results for even sized clusters [16,34], present TB calculation overestimates the HOMO-LUMO gap, but the size dependent behaviour of gaps and magic effects are qualitatively reproduced.

3.5 Ionization potentials

The present TBMD formalism can only be relied on to give qualitative results on the variation of the ionization potential with cluster size. This is because the set of SK-TB parameters in this scheme implies that the expected ionization energy for small clusters to be approximately (by Koopman's theorem) is equal to the on-site energy E_s, which is usually higher than the highest occupied s-orbital energy for free atom [20]. This may be improved by the proposed scaling scheme of Cohen. Mehl and Papaconstantopoulos [36]. In Figure 7 we present the present results for Cu_n clusters with $n \leq 24$. We found even-odd alternation due to electron pairing along with high peaks due to the electronic shell closing for Cu_2, Cu_8, Cu_{18} and Cu_{20}.

4 Conclusion

Tight-binding molecular dynamics scheme has been used to obtain ground state structures, binding energies, relative stabilities, HOMO-LUMO gaps as well as ionization potentials of Cu_n clusters for $n \leq 24$. We have fitted the parameters of the present TB scheme from our previous *ab initio* [10] calculation. We made an extensive comparison with various *ab initio* calculations and available experimental results, which shows very good agreement. For very small clusters, up to Cu_5, we found planer structures which are in agreement with experiment [16]. d-states have least effect for very small clusters $n \leq 5$, while d states start playing an important role as size grows. Calculated binding energies are in good agreement with the LDA based *ab initio* calculations, but overestimates it from the TCID experimental value as shown in Table 2 and Figure 4. This is simply because we fitted the parameters in the present scheme from the LDA based *ab initio* calculation, where this kind of overestimation in binding energy is inherent.

Prominent electronic shell closing effect is observed for Cu_2, Cu_8, Cu_{18} and Cu_{20}, which correspond the magic numbers. Due to electron pairing effect even-odd alternation is found in relative stabilities, HOMO-LUMO gap energies and ionization potential. Using Gupta potential, Darby et al. found significant high peaks in the relative stability for $n = 7$, 13, 19, 23, due to icosahedral or polyicosahedral growth. However, in the present study we have not got any such peaks for those clusters except Cu_{13}. Due to the peak causing from the even-odd alternation

for $n = 6$ and significant high peak causing from the electronic shell closing for $n = 8$, the peak for $n = 7$ due to the structural effect is suppressed. Due to the peaks causing from electronic shell closing for $n = 18$ and 20, the peak at $n = 19$ due to double icosahedral structure is not found. Similarly, for the average even-odd alternation peaks at $n = 22$ and 24, the peak for $n = 23$ for poly-icosahedral growth is not found. Therefore, we conclude that the electronic effects, electron pairing and electronic shell closing, dominates over the geometrical effect for copper cluster. The computational efficiency of the present scheme readily allows us to do an unrestricted search for ground state geometry for larger clusters.

This work is partially supported by the School of Engineering, University of Warwick, UK.

References

1. W.A. de Heer, Rev. Mod. Phys. **65**, 611 (1993)
2. M. Brack, Rev. Mod. Phys. **65**, 677 (1993)
3. See, e.g., *Physics and Chemistry of Small Clusters*, edited by P. Jena, B.K. Rao, S.N. Khanna (Plenum Press, New York, 1987); *Elemental and Molecular Clusters*, edited by G. Benedek, T.P. Martin, G. Pacchioni (Springer-Verlag, Berlin, 1988); *Clusters of Atoms and Molecules,* edited by H. Haberland (Springer-Verlag, Heidelberg, 1994), Vols. 1 and 2
4. G. Apai, J.F. Hamilton, J. Stohr, A. Thompson, Phys. Rev. Lett. **43**, 165 (1979)
5. A. Balerna, E. Bernicri, P. Piccozi, A. Reale, S. Santucci, E. Burrattini, S. Mobilio, Surf. Sci. **156**, 206 (1985)
6. P.A. Montano, H. Purdum, G.K. Shenoy, T.I. Morrison, W. Schultze, Surf. Sci. **156**, 216 (1985)
7. P. Calaminici, A.M. Köster, N. Russo, D.R. Salahub, J. Chem. Phys. **105**, 9546 (1996)
8. C. Massobrio, A. Pasquarello, R. Car, Chem. Phys. Lett. **238**, 215 (1995)
9. H. Akeby, I. Panas, L.G.M. Pettersson, P. Seigbahn, U. Wahlgren, J. Chem. Phys. **94**, 5471 (1990)
10. M. Kabir, A. Mookerjee, R.P. Datta, A. Banerjea, A.K. Bhattacharya, Int. J. Mod. Phys. B **17**, 2061 (2003)
11. G. D'Agostino, Philos. Mag. B **68**, 903 (1993)
12. R.P. Gupta, Phys. Rev. B **23**, 6265 (1983)
13. S. Darby, T.V. Mortimer-Jones, R.L. Johnston, C. Roberts, J. Chem. Phys. **116**, 1536 (2002)
14. B.J. Winter, E.K. Parks, S.J. Riley, J. Chem. Phys. **94**, 8618 (1991)
15. K.J. Taylor, C.L. Pettiette-Hall, O. Cheshnovsky, R.E. Smalley, J. Chem. Phys. **96**, 3319 (1992)
16. J. Ho, K.M. Ervin, W.C. Lineberger, J. Chem. Phys. **93**, 6987 (1990)
17. I. Katakuse, T. Ichihara, Y. Fujita, T. Matsuo, T. Sakurai, H. Matsuda, Int. J. Mass Spectrom. Ion Proc. **67**, 229 (1985); Int. J. Mass Spectrom. Ion Proc. **74**, 33 (1986)
18. V.A. Spasov, T.H. Lee, K.M. Ervin, J. Chem. Phys. **112**, 1713 (2000)
19. M. Menon, K.R. Subbaswamy, Phys. Rev. B **47**, 12754 (1993); Phys. Rev. B **50**, 11577 (1994); Phys. Rev. B **51**, 17952 (1996)
20. N. Lathiotakis, A. Andriotis, M. Menon, J. Connolly, J. Chem. Phys. **104**, 992 (1996)
21. A. Andriotis, M. Menon, Phys. Rev. B **57**, 10069 (1998)
22. M. Kabir, A. Mookerjee, A.K. Bhattacharya, Phys. Rev. A **69**, 043203 (2004)
23. J.C. Slater, G.F. Koster, Phys. Rev. **94**, 1498 (1954)
24. W.A. Harrison, *Electronic Structure and the Properties of Solids* (Dover, 1989)
25. D. Tomaǹek, M. Schluter, Phys. Rev. B **36**, 1208 (1987)
26. K.P. Huber, G. Herzberg, *Molecular Spectra and Molecular Structure* (Van Nostrand-Reinhold, New York, 1989), Vol. IV
27. N. Aslund, R.F. Barrow, W.G. Richards, D.N. Travis, Ark. Fys. **30**, 171 (1965)
28. C.W. Bauschlicher Jr, S.R. Langhoff, H. Partridge, J. Chem. Phys. **91**, 2412 (1989); C.W. Bauschlicher Jr, Chem. Phys. Lett. **156**, 91 (1989)
29. U. Lammers, G. Borstel, Phys. Rev. B **49**, 17360 (1994)
30. Y. Wang, T.F. George, D.M. Lindsay, A.C. Beri, J. Chem. Phys. **86**, 3593 (1987); D.M. Lindsay, L. Chu, Y. Wang, T.F. George, J. Chem. Phys. **87**, 1685 (1987)
31. S. Darby, T.V. Mortimer-Jones, R.L. Johnston, C. Roberts, J. Chem. Phys. **116**, 1536 (2002)
32. J. Zhao, Y. Luo, G. Wang, Eur. Phys. J. D **14**, 309 (2001)
33. E.K. Parks, L. Zhu, J. Ho, S.J. Riley, J. Chem. Phys. **102**, 7377 (1995)
34. C.L. Pettiette, S.H. Yang, M.J. Craycraft, J. Conceicao, R.T. Laaksonen, O. Cheshnovsky, R.E. Smalley, J. Chem. Phys. **88**, 5377 (1998)
35. O.B. Christensen, K.W. Jacobsen, J.K. Norscov, M. Mannien, Phys. Rev. Lett. **66**, 2219 (1991)
36. R.E. Cohen, H.J. Mehl, D.A. Papaconstantopoulos, Phys. Rev. B **50**, 14694 (1994)